Video Article

# Two Algorithms for High-throughput and Multi-parametric Quantification of *Drosophila* Neuromuscular Junction Morphology

Anna Castells-Nobau*[1], Bonnie Nijhof*[1], Ilse Eidhof[1], Louis Wolf[2], Jolanda M. Scheffer-de Gooyert[1], Ignacio Monedero[3,4], Laura Torroja[3], Jeroen A.W.M. van der Laak[2,5], Annette Schenck*[1]

[1]Department of Human Genetics, Donders Institute for Brain, Cognition and Behaviour, Radboud University Medical Center

[2]Microscopical Imaging Centre (MIC), Radboud University Medical Center

[3]Department of Biology, Universidad Autónoma de Madrid

[4]Department of Clinical and Experimental Medicine, Linköping University

[5]Department of Pathology, Radboud University Medical Center

*These authors contributed equally

Correspondence to: Annette Schenck at Annette.Schenck@radboudumc.nl

URL: https://www.jove.com/video/55395
DOI: doi:10.3791/55395

Keywords: Neuroscience, Issue 123, Fiji, *Drosophila*, NMJ, macro, synapse, image segmentation, morphometry

Date Published: 5/3/2017

Citation: Castells-Nobau, A., Nijhof, B., Eidhof, I., Wolf, L., Scheffer-de Gooyert, J.M., Monedero, I., Torroja, L., van der Laak, J.A., Schenck, A. Two Algorithms for High-throughput and Multi-parametric Quantification of *Drosophila* Neuromuscular Junction Morphology. *J. Vis. Exp.* (123), e55395, doi:10.3791/55395 (2017).

## Abstract

Synaptic morphology is tightly related to synaptic efficacy, and in many cases morphological synapse defects ultimately lead to synaptic malfunction. The *Drosophila* larval neuromuscular junction (NMJ), a well-established model for glutamatergic synapses, has been extensively studied for decades. Identification of mutations causing NMJ morphological defects revealed a repertoire of genes that regulate synapse development and function. Many of these were identified in large-scale studies that focused on qualitative approaches to detect morphological abnormalities of the *Drosophila* NMJ. A drawback of qualitative analyses is that many subtle players contributing to NMJ morphology likely remain unnoticed. Whereas quantitative analyses are required to detect the subtler morphological differences, such analyses are not yet commonly performed because they are laborious. This protocol describes in detail two image analysis algorithms "*Drosophila* NMJ Morphometrics" and "*Drosophila* NMJ Bouton Morphometrics", available as Fiji-compatible macros, for quantitative, accurate and objective morphometric analysis of the *Drosophila* NMJ. This methodology is developed to analyze NMJ terminals immunolabeled with the commonly used markers Dlg-1 and Brp. Additionally, its wider application to other markers such as Hrp, Csp and Syt is presented in this protocol. The macros are able to assess nine morphological NMJ features: NMJ area, NMJ perimeter, number of boutons, NMJ length, NMJ longest branch length, number of islands, number of branches, number of branching points and number of active zones in the NMJ terminal.

## Video Link

The video component of this article can be found at https://www.jove.com/video/55395/

## Introduction

Cognitive disorders such as intellectual disability, autism spectrum disorder and schizophrenia are often characterized by abnormal synaptic function[1,2,3]. Synapse morphology and function are tightly intertwined; morphological defects can cause synaptic malfunction and, reversely, aberrant synaptic transmission will impact synaptic maturation and morphology[4,5,6].

A number of model organisms have been employed in order to better understand synapse biology and shed light on how synaptic changes affect brain function in health and disease[7,8,9]. The *Drosophila* NMJ is an extensively studied and well-established *in vivo* model for glutamatergic synapse biology[10,11]. In the past decades, this model has been used for physiological and gene-focused studies, as well as for large scale genetic screens, with the aim to detect morphological differences between NMJs. In particular, forward genetic screens have identified many crucial regulators and mechanisms underlying synapse development and function[12,13,14,15,16]. However, most of these screens relied on visual assessment of NMJ terminal morphology and on qualitative detection of the synaptic abnormalities or semi-quantitative scoring of few morphological features. As a consequence, rather subtle synaptic morphological abnormalities that are non-obvious to the human eye are easily missed. In order to be able to comprehensively detect quantitative differences, the NMJ has to be accurately evaluated by systematic quantification of the morphological parameters of interest. Measuring NMJ features manually is laborious, especially when there are several NMJ features of interest and/or when performing large-scale genetic screenings. In order to support multiparametric, high-throughput morphological analysis and to achieve objective quantification, two macros "*Drosophila* NMJ Morphometrics" and "*Drosophila* NMJ Bouton Morphometrics" were developed[17]. Both macros run in the open source image analysis software Fiji[18], and enable quantification of both confocal and nonconfocal images.

*"Drosophila* NMJ Morphometrics" measures NMJ terminals immunostained with the postsynaptic marker disc large-1 (Dlg-1) or the presynaptic horseradish peroxidase (Hrp), co-labeled with the active zone marker bruchpilot (Brp). It quantifies nine morphological parameters (further described below): NMJ area, NMJ perimeter, number of boutons, NMJ length, NMJ longest branch length, number of islands, number of branches, number of branching points and number of active zones in the synaptic terminal (**Figure 1**). Although an algorithm for determining the number of boutons is present in this macro, it did not meet the criteria for accuracy[17]. To properly assess the number of boutons, it is necessary to use the "*Drosophila* NMJ Bouton Morphometrics" macro, which is specifically designed to quantify boutons using NMJ preparations immunostained by anti-Synaptotagmin (Syt) or anti-Cysteine string protein (Csp), and co-immunolabeled with Brp. The *"Drosophila* NMJ Bouton Morphometrics" macro quantifies the following parameters: number of boutons, NMJ bouton area, NMJ length, NMJ longest branch length, number of islands, number of branches, number of branching points and number of active zones (**Figure 2**).

The macros consist of 3 sub-macros: **(I)** "Convert to stack" identifies all available image files and creates Z-hyperstacks and maximum intensity projections of both channels. As output, this macro will generate two new files per synapse called "stack_image_name" and "flatstack_image_name". **II)** "Define ROI" will open all maximum projection images "flatstack_image_name" consecutively and present them with the request to manually define the region of interest (ROI) in which the specific synaptic terminal of interest is present. This was implemented to allow exclusion of synapses connecting to adjacent muscles and/or other types of synaptic terminals (such as 1s) that can be present in the images[11]. **(III)** "Analyze" applies fully automated analysis to the image area within the borders of the ROI. As a result of this step, the user will obtain two new files: "results.txt" where all the numerical measurement will be annotated and a "res_image_name.tif" where the underlying image segmentations produced by the macro will be illustrated. During image analysis three structures are derived from each synaptic terminal: the NMJ outline, the NMJ skeleton, and the number of Brp-positive active zones. The NMJ outline is used to determine the NMJ area and its perimeter and a subsequent watershed separation provides the number of boutons. From the skeleton, five NMJ features are deduced: the total NMJ length, the sum of the length of the longest continuous path connecting any two end points (longest branch length), the number of unconnected compartments per NMJ (referred to as "islands"), the number of branches, and the number of branching points (one branching point connects three or more branches). The number of active zones is determined in the Brp-channel by counting Brp-positive spots. The annotated NMJ outline (yellow line), the NMJ skeleton (blue line), and the number of Brp-positive active zones (indicated by white foci) are displayed in a results picture and the measurements of the parameters are processed to an (.txt) output file (**Figure 3**).

*Drosophila* NMJ Morphometrics" and "*Drosophila* NMJ Bouton Morphometrics" were first described and extensively validated by Nijhof *et al.*[17]. This manuscript focuses on the methodology to analyze NMJ morphology using the macros "*Drosophila* NMJ Morphometrics" and "*Drosophila* NMJ Bouton Morphometrics". Prior to macro-assisted analyses, NMJ dissections and immunostainings need to be performed. These are crucial steps, and the combination of markers used for immunohistochemistry needs to be suitable for macro analyses. These steps are briefly mentioned in section 1 of this protocol and direct the user to references describing in detail the protocols to execute these procedures.

## Protocol

# 1. Requirements Prior to Image Processing

1. Perform *Drosophila* open book preparations of third instar wandering larvae (L3), as previously described[19].
2. Co-immunolabel *Drosophila* NMJ terminals using a combination of two markers: Dlg-1 or Hrp together with Brp for analysis with "*Drosophila* NMJ Morphometrics", and Syt or Csp together with Brp for analysis with "*Drosophila* NMJ Bouton Morphometrics"[20].
   NOTE: Antibodies from the same species can be combined by pre-labeling one with an antibody-conjugation kit such as the Zenon Alexa Labeling Kits[17].
3. Image NMJ terminals using a microscope of choice, *e.g.,* fluorescence (with or without ApoTome) or confocal microscopy.
   1. Acquire a 2-channel image stack of the NMJ terminal.
      1. Adjust the microscope settings in a manner that channel 1 acquires the NMJ terminal immunolabeled with Dlg-1 (or Hrp, Syt, Csp) and channel 2 the NMJ terminal immunolabeled with Brp.
      2. Optionally, analyze one-channel images (of synapses immunolabeled with a single antibody) with the macros. Image NMJs immunolabeled uniquely with Dlg-1 or Hrp for analysis with "*Drosophila* NMJ Morphometrics", or Syt or Csp for "*Drosophila* NMJ Bouton Morphometrics".
         NOTE: It is not possible to analyze synapses immunostained with only anti-Brp.
   2. Export the obtained images as individual '.tiff files. Invert the channel order prior to running the macros if not acquired as indicated.

# 2. Software Requirements and Installation

1. Download the macros: "*Drosophila* NMJ Morphometrics" and "*Drosophila* NMJ Bouton Morphometrics" from the following website: https://doi.org/10.6084/m9.figshare.2077399.v1[21].
2. Move the cursor to the folder "Macros update 1", and click on the appearing option "view". A list with the content of this folder will appear. The folder contains the macros "*Drosophila* NMJ Morphometrics" and "*Drosophila* NMJ Bouton Morphometrics".
   NOTE: Both macros are compatible with Fiji versions 1.4, which is also provided in the same folder. The macros may not run on recent versions. Please utilize the provided version 1.4. It is unproblematic to start this version, even on computers with a more recent Fiji version available.
3. Click on "Download all". The folder content will be downloaded to the computer as a .zip file. Unzip the downloaded file.
4. Copy the *Drosophila*_NMJ_Morphometrics.ijm and *Drosophila*_NMJ_Bouton Morphometrics.ijm files to Fiji.app/plugins/ directory. When restarting the program, the macros will appear at the bottom of the Plugins dropdown menu.

## 3. Run Sub-macro "Convert to Stack" to Create Z-projections and Hyperstacks of the NMJ Images

1. Start the graphical interface by selecting Plugins in the toolbar and choose "*Drosophila* NMJ Morphometrics" in the dropdown menu.
2. Define the "Unique File String" setting in the macro's graphical interface.
   NOTE: The microscope software uses an identification signature to organize planes and channels when storing stacks as individual '.tiff files. The entered unique file string setting needs to specify the signature assigned by the software to the first plane of the first channel (important: lowest plane and channel number needs to be indicated).
3. Select only the sub-macro "Convert to stack" and click "ok" and select the folder where the images are located. If a main directory with several subfolders is selected, all individual '.tiff files within the main directory and subfolder matching the unique file string criteria will be processed.
   1. If the z-stack only contains one channel, select the box "Channel 1 only".
4. Notice that two new files per NMJ image, by default termed as stack_image_name and flatstack_image_name will appear. Store only these stack and flatstack for further analysis. The .tiff file series can be deleted at this point, minimizing the required storage capacities and avoiding potential error sources.

## 4. Run Sub-macro "Define ROI" to Delineate the NMJ Terminal of Interest

1. Start the graphical interface of "*Drosophila* NMJ Morphometrics".
2. Select only the checkbox "Define ROI" and press "OK" and select the main directory where the images entitled flatstack_name are stored and press "Select". The sub-macro "Define ROI" automatically searches through all subfolders within the selected main directory.
3. As the first projection opens, select the "Freehand selections" tool in the toolbar.
4. Using the mouse draw a selection that exclusively contains the complete NMJ terminal of interest and click "OK" in the window "Define terminal". The macro will proceed with the next projection.
5. Delineate the next ROI and repeat until all ROIs are defined. The ROI image file, named "roi_image_name", will be stored in the same directory as the previously generated stack and projection images for each of the processed images. The output of this sub-macro is a binary image of the ROI in white on a black background.

## 5. Run Sub-macro "Analyze" to Quantify NMJ Terminal Features

1. Go to the toolbar, select "Plugins" and use:
   "*Drosophila*_NMJ_Morphometrics" when analyzing synapses immunolabeled with anti-Dlg-1 or anti-Hrp (channel 1) together with anti-Brp (channel 2), or "*Drosophila*_NMJ_Bouton_Morphometrics" when analyzing synapses immunolabeled with anti-Syt or anti-Csp (channel 1) together with Brp (channel 2).
   1. When one channel image stacks are to be analyzed (the structural channel Dlg-1 or HRP for *"Drosophila*_NMJ_Morphometrics", or Syt or Csp for "*Drosophila*_NMJ__Bouton_Morphometrics"), select the box "Channel 1 only".
2. Adjust the scale corresponding to the images to be analyzed.
   1. If one pixel in the image corresponds to 2.5 µm, indicate Scale-Pixels = 1, Scale-Distance in µm = 2.5. In case both settings are left at 0, the NMJ area, perimeter, length and longest branch length will be expressed in number of pixels.
3. If required, adjust the default analysis settings of the macro. Perform adjustments only if the sub-macro “Analyze” has previously been run with unsatisfactory results (see end of this section, and section 6 for instructions how to optimize the settings).
4. Select the checkboxes "Analyze" and "Wait" and press "OK".
   1. Select the "Wait" check box when running the sub-macro "Analyze" on 2 channel images. Otherwise errors in active zone counting can occur due to limited computer capacities .
5. As a new window "Choose a Directory" opens, select the directory where the images are located and press "select". The macro will analyze all images stored in the main directory and, if applicable, subsequent folders (using the three files from executing the previous sub-macros: stack_image_name, flatstack_image_name and roi_image_name). The macro processes each image individually and consecutively. This can take several minutes per image stack (depending on the computer capacity).
6. After running the macro, note that a new image file named res_image_name for each analyzed synapse stored will be created in the parental folder. The quantitative measurements will be stored as "results.txt" file.
7. Inspect all result images to detect and exclude pictures with segmentation errors. Possible segmentation errors are described in **Table 3**, along with advice how to adjust settings to circumvent these errors. Result images with such segmentation errors are provided as examples in **Figure 4**.
   NOTE: When running the macro with the default settings observed in the user interface, there was an accuracy of approximately 95% when macro assessment was compared to manual evaluation[17].

## 6. Adjust the Macro Settings to the Images

1. When more than 5% of images show segmentation errors, explore the different algorithms to define/choose the most suitable macro settings for the images.
2. **Adjust rolling ball radius value**

NOTE: The rolling ball radius function subtracts the background of the image. This function is of crucial importance when working with images acquired on fluorescence microscopes and/or when images have high background noise. The subtraction of the background will help the macro's auto-thresholding steps to produce adequate segmentation of the NMJ terminals.

1. Select three NMJ stack_image_name images generated by the sub-macro “Convert to stack”. Choose images which are representative for the image dataset.
2. In the toolbar, select Image | Color | Split channels. Two image stacks will be created, one representing channel 1 and the other channel 2, respectively and save them.
3. Open the image stack belonging to channel 1 open, corresponding to Dlg-1, Hrp, Syt or Csp immunolabeling.
4. Run the filter "Subtract background" by selecting "Process" in the toolbar followed by "Subtract Background…" in the dropdown menu.
5. Click on the preview checkbox in the pop-up window and adjust the rolling ball radius to the value most appropriate for the images. The “Rolling ball radius” setting should be adjusted to values that increase the contrast between synapse and background (see **Figure 5A**').
    1. See **Figure 5** for an example. In panel A, parts of the synapse show the same grey levels as the background, whereas in **Figure 5** panel A' a “Rolling ball radius” of 500 results in strong contrast between the synapse and the background.
6. Create a z-projection by selecting in the toolbar Image | Stack| Z-projection, chose Projection type = Max Intensity and save the resulting image. When the appropriate value for the rolling ball radius is defined, run the “Subtract background” algorithm on the remaining representative images with the same rolling ball radius value. Create the Z-projections and save them (in any directory).
   NOTE: The rolling ball radius value for 8-bit or RGB images should be at least as large as the radius of the largest object in the image that is not part of the background. For 16-bit and 32-bit images the radius should be inversely proportional to the pixel value range[22].

3. **Determine the different auto-thresholds that will be used**
    1. Open the Z-projections saved in the previous step (6.2.6) and Select Image | Adjust | AutoThreshold | Try all.
    2. As a binary thresholded result image will appear with all different auto-threshold algorithms, determine the most suitable algorithm for the images.
        1. When running the macro later on, change the threshold in the macro settings accordingly.
        2. Use more restrictive thresholds such as "RenyiEntrophy" or "Moments" as the NMJ outline threshold and more permissive thresholds such as "Li" to determine the NMJ skeleton, and "Huang" to determine active zones. When images are very sharp with little to no background, use "Huang" as" NMJ outline threshold. Otherwise parts of the synapse might be missing after image segmentation.
        3. See **Figure 5B** for an example. Appropriate segmentation of the synapse is obtained with auto-thresholds highlighted by green boxes. Some examples of non-suitable thresholds are highlighted by red boxes (check synapses at high magnification). In the latter, either parts of the synapse are missing or parts of the background are included. See reference 23 for more information.

4. **Determine the maximum size of the small particles**
   NOTE: This function will exclude all particles detected by the NMJ outline threshold and Skeleton threshold that are smaller than the defined value in the "small particles setting" from the analysis. This value is defined in pixels. This function serves as a noise filter and is very useful when high rates of non-uniform background (such as crystals/dust) are present in the obtained images.
    1. Open the Z-projections saved in step 6.2.6. and set the scale to detect number of pixels via Analyze | Set Scale. Apply the following settings: distance in pixels=1, known distance=1, pixel aspect ratio=1, Unit of length=pixel and press "Ok". Click on the "Oval selection" tool in the toolbar.
    2. Using the mouse draw a selection closely surrounding single particles that are present in the immunostaining but do not belong to the NMJ. Press Ctrl+m for a Windows user or cmd+m for Mac users. A result window will open, indicating the area of the particles selected in number of pixels.
    3. Repeat the previous step several times with several artifacts present in the images to determine the biggest contaminating particle/ artifact area. This will be the value to set in the setting when running the macro later on. When running the macro set the "Small Particles Size" as the smallest particle size observed pus a margin of 25%.
    4. See **Figure 5D** for an example. The biggest crystal detected has an area of 112 pixels. The "Small particles size" setting, when processing this image with the macro, should be set to 125 - 150.

5. **Determine minimum bouton size**
   NOTE: This function will exclude all boutons detected by the NMJ outline threshold that are smaller than the defined value from the analysis. This value is defined in pixels.
    1. Follow the same steps as described in section 6.4, but in this case draw a selection surrounding the smallest boutons present in the NMJ terminal. Choose the smallest area corresponding to the smallest bouton of the measured ones. This is the value to set in the minimum bouton size setting when running the macro later on.

6. **Define "Maxima noise tolerance" value**
    1. To define the “Find maxima noise tolerance” value for the macro, open the channel 2 Z-stack saved in section 6.2.2.
    2. Go to the plugins tab in the popup menu, select Process | Maximum(3D), and when the maximum_image_name appears (which can take up a few minutes), close the original image stack.
    3. Select the Maximum…_image_name (the newly obtained image stack) and select Plugins | Process | Minimum (3D), when the new image Minimum of Maximum…_image_name apears close the Maximum … _image_name stack.
    4. In the toolbar, select Process | Find maxima…. A new window "Find maxima…" will open. Click the checkbox "Preview point selection…" and fill the "Noise tolerance" box with the default macro setting 50. The maxima points will be indicated in the image as little crosses.
        1. Increase the “Noise tolerance” value if observing an excess of annotated active zones, i.e. crosses that are not on top of active zones that are not in focus on the selected stack plane, or false active zones that are detected in the background.

1. On the other hand, if observing incompletely annotated active zones, i.e. active zones in focus not being recognized, decrease the “Maxima noise tolerance” value. Keep trying different values following this procedure till the crosses are appropriately labeling active zones in focus. Fill the “Find maxima noise tolerance” with this value.
2. See **Figure 5C** for an example. Too many active zones are detected. In **Figure 5C**’ only the active zones in focus are detected when increasing the “Maxima noise tolerance” value.

5. Run the sub-macro "Analyze" for the representative images selected in step 5.1, with the settings defined in the all the previous steps.

7. **Adjust Brp-puncta lower and upper threshold**
   1. Notice that a new file will be appearing after running the macro according to step 6.6, called 2_active_zone_stack_image_name. In this image stack the active zones detected by the "Find maxima" function are indicated by white dots in each plane.
   2. Open this file by dragging and dropping it into the toolbar and select Image | Stack | Z-project | Projection type = Sum slices. A projection of the 2_active_zone_stack_image_name will be obtained.
   3. Select Image | Adjust | Threshold. A new window "Threshold" will open. Slide the upper bar to choose a threshold value where, all desired foci/Brp-positive spots are visualized in red.
      NOTE: If the threshold is set too low, an excess of active zones will be counted. If set too high, a fraction of the active zones will be missed.
      1. See **Figure 5E** for an example. When threshold is set to 400, most of the active zones (symbolized as a 1 pixel foci) are not included in the segmentation, since they are not highlighted in red (**Figure 5E**). When threshold is set to a value of 50 all the active zones are highlighted in red (**Figure 5E**’).
   4. Define this value as minimum threshold. Leave “Upper puncta threshold” on the maximum value.
   5. Re-run the sub-macro “Analyze” for the representative images with the settings defined in all the previous steps of this section. Critically evaluate the resulting image files and make sure that the segmentation is done properly. If this is not the case readjust the settings according to the nature of the segmentation errors (**Figure 4**, **Table 3**).

## Representative Results

The text results file will appear in the main directory. It summarizes all the measured parameters per image. The results are linked to the file name and the parameters are subsequently summarized in the order indicated in **Tables 1 and 2.**

Res_image_name is a three-image stack. The first image highlights the outline and skeleton of the NMJ terminal determined by the macro based on channel 1 (immunolabeling Dlg-1, Hrp, Syt, or Csp). The second image is a copy of the first image and additionally shows the identified Brp-positive spots that are detected in channel 2 as schematized foci. The third image provides the maximum projection of the second channel together with identified Brp-positive foci.

The NMJ outline threshold is represented in yellow in the macro output result image. NMJ area, perimeter and number of boutons are deduced from this threshold.

The NMJ skeleton threshold is represented in blue in the macro output result image. NMJ length, longest branch length, number of branches, branching points and islands are deduced from this threshold.

The NMJ Active zones threshold is not represented in the macro output result image. This threshold determines the area where the Brp-positive foci potentially could be encountered by the macro. It is meant to create an NMJ area that is slightly bigger than the one defined by the NMJ outline threshold. When a too restrictive threshold is selected, Brp-positive foci located at the margin of the synapse may be excluded. When the threshold is too permissive, background noise may be counted as Brp-positive spots (**Figures 1 - 2**).

To validate the performance of the "*Drosophila* NMJ Morphometrics" macro, three mutant conditions that were already described to present synaptic defects in different NMJ parameters were tested. Each defect was detected by a different image segmentation procedure performed by the macro (NMJ outline, skeleton or active zones, respectively[17]). After targeting the three genes of interest by inducible RNAi and performing dissections and NMJ immunostaining of L3 larvae, the macro was run. The obtained NMJ morphological measurements were then pairwise (RNAi versus its control) compared using a t-test. In all three cases, statistical differences were found between mutants and controls affecting parameters that are in agreement with the previously reported morphological defects. This confirms that the macros are indeed able to adequately identify previously described defects at the *Drosophila* NMJ.

*Ankyrin* 2 (*Ank2*, CG42734) mutants are known to show synaptic morphology defects, including fused boutons and smaller NMJs. These defects were observed for *Ank2* mutants[24,25] and *Ank2* knockdown flies[26]. NMJ terminals of pan-neuronal *Ank2*-RNAi knockdown flies (*w;UAS-Dicer-2/UAS-Ank2 RNAi KK107238;elav-Gal4/+*) showed significantly smaller NMJ area (mean = 339.25 $\mu m^2$; t-test p = 2.18 x $10^{-8}$) and perimeter (mean = 238.24 µm; t-test p = 1.82 x $10^{-3}$), compared to the genetic background control dataset (*w;UAS-Dicer-2/UAS-KK60100;elav-Gal4/+*) (mean = 451.95 $\mu m^2$ and mean = 288.62 µm, respectively) after running "*Drosophila* NMJ Morphometrics" (**Figures 6A & 4B**).

The GTPase *Rab3* (CG7576) is required for proper bruchpilot distribution and the *rup* mutant presents with a significantly reduced number of active zones[27]. A significant decrease in the number of active zones was observed when measuring Brp-positive foci by the "*Drosophila* NMJ Morphometrics" macro in NMJ terminals of pan-neuronal *Rab3* knockdown flies (*w;UAS-Dicer-2/UAS-RNAi KK100787;elav-Gal4*) . The average number of active zones per NMJ terminal in *Rab3*-RNAi was 138 in contrast to 290 detected in the control dataset (*/+*) t-test p = 4.43 x $10^{-29}$) (**Figures 6A & 4C**).

*Highwire* (*hiw*, CG32592) is an important regulator of NMJ growth; mutations in *hiw* gene lead to overgrow and extended branching of the NMJ terminals[28]. Measuring NMJ terminals of pan-neuronal *Hiw*-RNAi knockdown line (*w;UAS-Dicer-2/UAS-RNAi-GD36085;elav-Gal4/+*) with "*Drosophila* NMJ Morphometrics", significant differences were observed in the skeleton-derived parameters: length (mean = 147.36 µm; control mean = 122.07 µm; t-test p = 7.31 x $10^{-7}$), longest branch length (mean = 122.19 µm; control mean = 105.65 µm; t-test p=4.62 x $10^{-4}$) number of branches (mean = 7.69; control mean = 5.74; t-test p = 2.52 x $10^{-2}$) and number of branching points (mean = 2.73; control mean = 1.79; t-test p = 3.31 x $10^{-2}$). All these parameters were significantly increased (120 - 180%) compared to the genetic background controls (*w;UAS-Dicer-2/UAS-GD60000;elav-Gal4/+*) (**Figures 6A & 4D**).

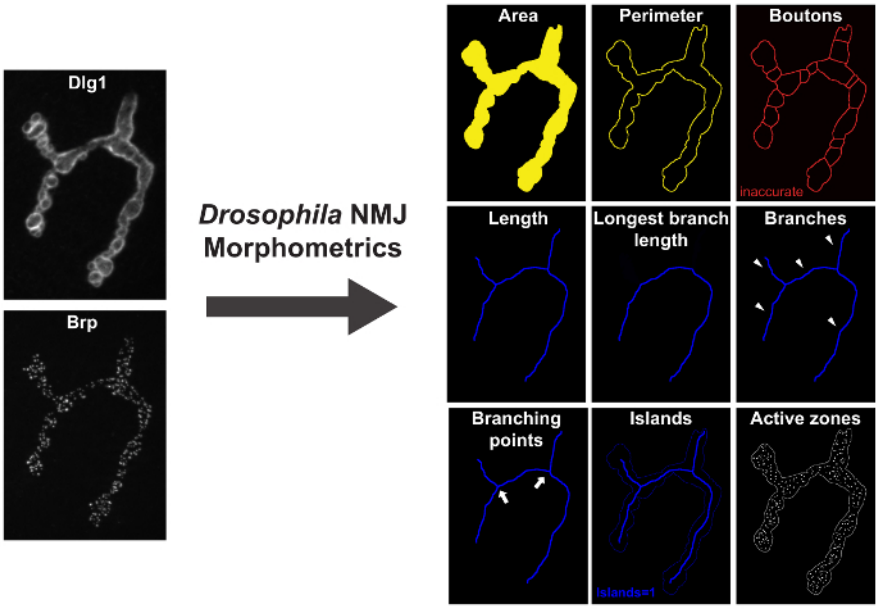


**Figure 1: *Drosophila*_NMJ_Morphometrics Measures 9 Parameters of the *Drosophila* NMJ.** On the left are Dlg-1 and Brp immunolabeled NMJ terminals, imaged on a fluorescence microscope with ApoTome. On the right are result images after running "*Drosophila* NMJ Morphometrics". Parameters area, perimeter and boutons are represented by the macro-annotated yellow outline indicated. Parameters length, longest branch length (LBL), branches, branching points, and islands are presented by the macro-annotated blue outline. Brp-immunolabeled foci (active zones) are represented by the macro as white spots in the result images. Please click here to view a larger version of this figure.

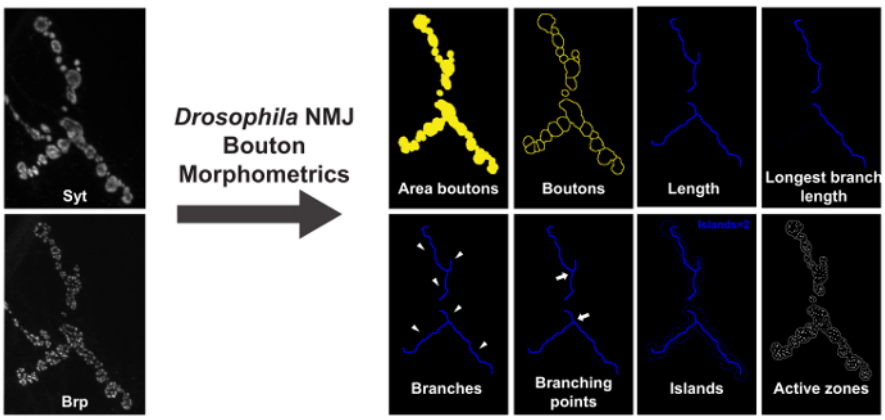


**Figure 2: *Drosophila* NMJ Bouton Morphometrics Measures 8 Parameters of the *Drosophila* NMJ.** On the left are Syt-1 and Brp immunolabeled NMJ terminal, imaged on a fluorescence microscope with ApoTome. On the right are result images after running "*Drosophila* NMJ Bouton Morphometrics". Parameters boutons and bouton area are represented by the macro-annotated yellow outline. Parameters length, longest branch length (LBL), branches, branching points, and islands are presented by the macro-annotated blue outline. Brp-immunolabeled foci (active zones) are represented by the macro as white spots in the result images. Please click here to view a larger version of this figure.

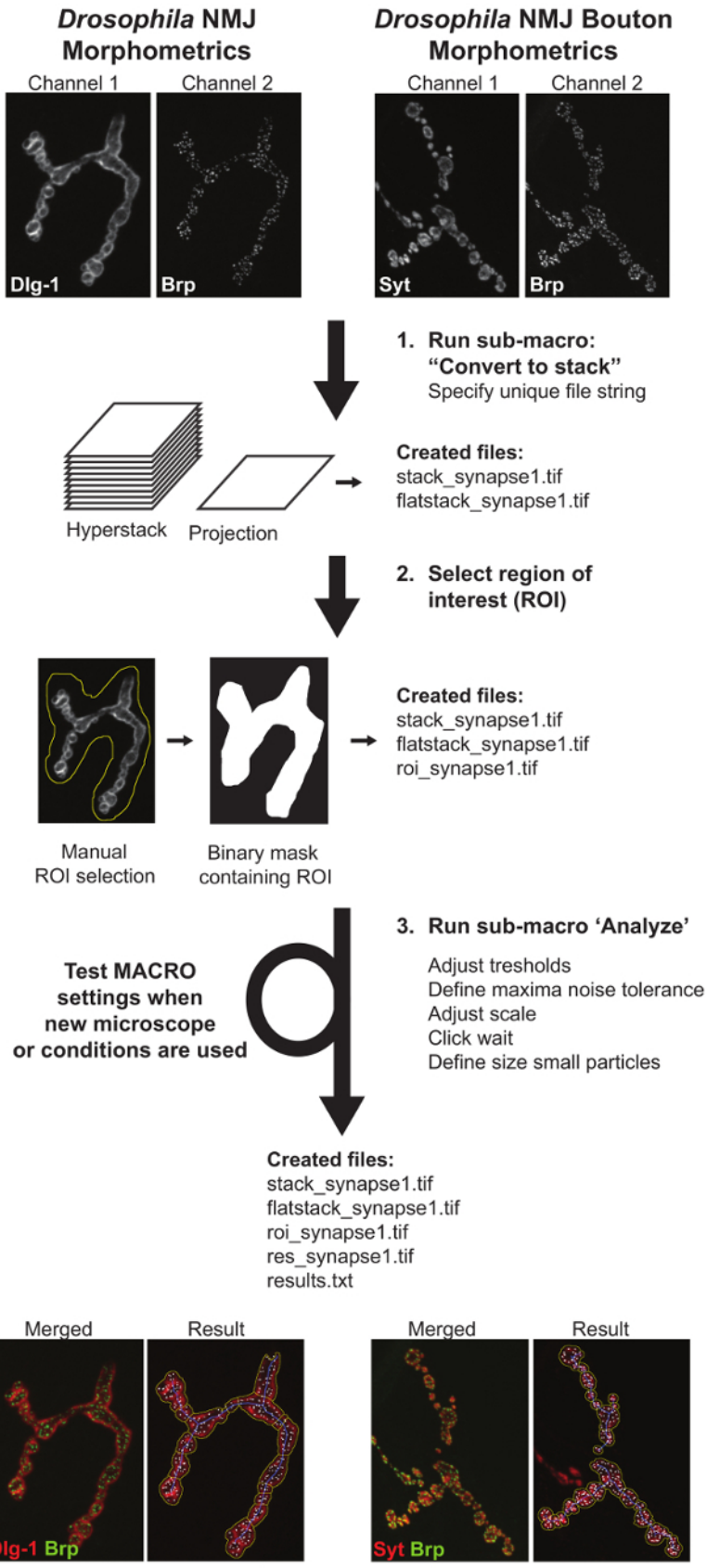

**Figure 3: Flow Chart Representing *Drosophila* NMJ Morphometrics and *Drosophila* NMJ Bouton Morphometrics Macros.** The first sub-macro "Convert to stack" creates projections and hyperstacks of the imaged NMJs. The second sub-macro "Define ROI" requires manual input defining the location of the NMJ terminal of interest. Sub-macro three, "Analyze", measures all NMJ parameters. A text file containing the quantitative values and a result image file depicting the parameter delineation are created to assist the user's evaluation of macro performance. When images are acquired under different conditions, the macro settings have to be tested and adjusted to ensure accurate analysis. Please click here to view a larger version of this figure.

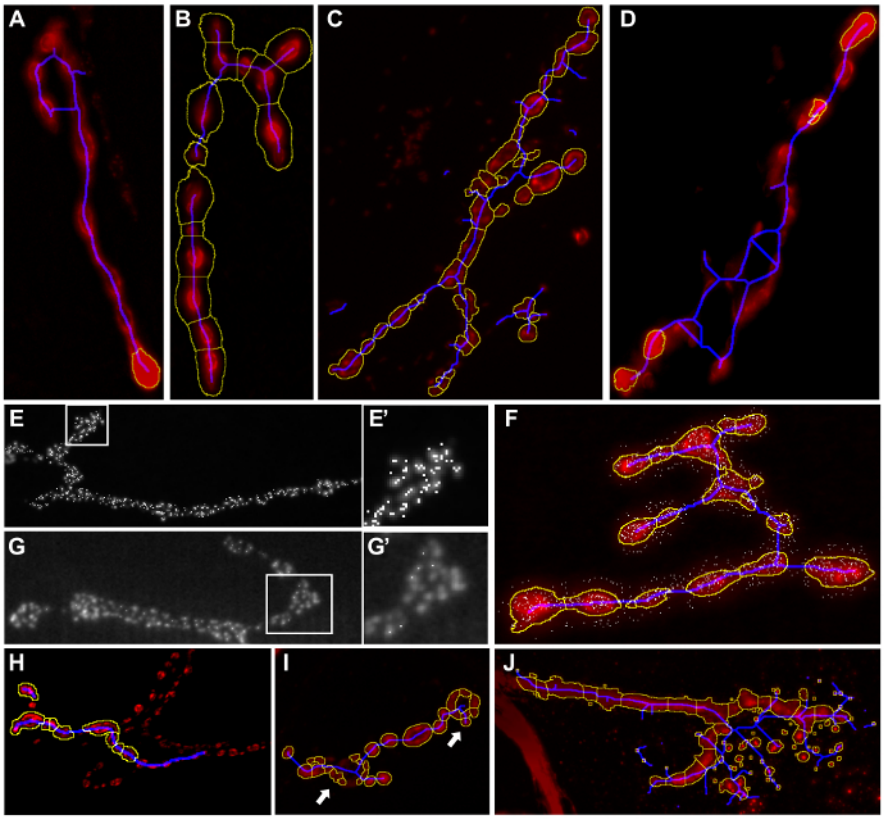


**Figure 4: Examples of Inappropriate Macro Segmentation Results.** Result images after running "*Drosophila* NMJ Morphometrics" or "*Drosophila* NMJ Bouton Morphometrics". Parts of the synaptic terminal are not included in the yellow outline (**A**). Parts of the background are included in the synaptic terminal by the yellow outline (**B**). Blue skeleton line extends beyond the synaptic terminal (**C - D**). Too many active zones are detected (**E - E'**). Some Active zones remain undetected by the analysis (**G - G'**). Active zones are detected outside the synapse (**F**). Incorrect bouton segmentation (Only applicable when running *Drosophila* NMJ Bouton Morphometrics), boutons are missed (**H**) or too many boutons are detected by the segmentation (**I**). Particles such a crystals or dust that are part of the background are included in the segmentation (**J**). Information how to change settings to avoid these errors are provided in **Table 3**. Please click here to view a larger version of this figure.

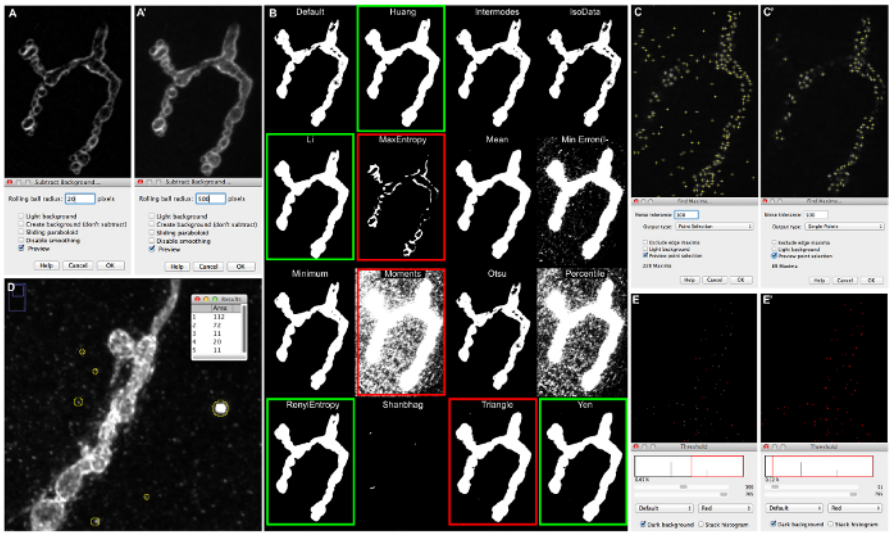


**Figure 5: Examples of Macro-setting Adjustments and Their Consequences for Image Segmentation.** (**A**) Subtract background preview of a Dlg-1 immunolabeled synapse, imaged on a fluorescence microscope with ApoTome, when "Rolling ball radius" is set to 20 (**A**) or 500 (**A'**). (**B**) Output images obtained after running Image | Adjust | Auto-Threshold | Try all the image illustrates image segmentations obtained by the 16 different auto-threshold algorithms. (**C**) "Find Maxima" preview when setting up "Noise tolerance" at 50 (**C**) and 500 (**C'**); Active zones that are detected by the segmentation are labeled by a small cross. (**D**) Measurement of the "small particles" appearing in the image background of a synapse immunolabeled with anti-Hrp, imaged on a confocal microscope. (**E**) "Sum slices" projection obtained from the 2_active_zone_stack_ima-ge_name. Threshold is set at 400 (**E**) and at 50 (**E'**). Please click here to view a larger version of this figure.

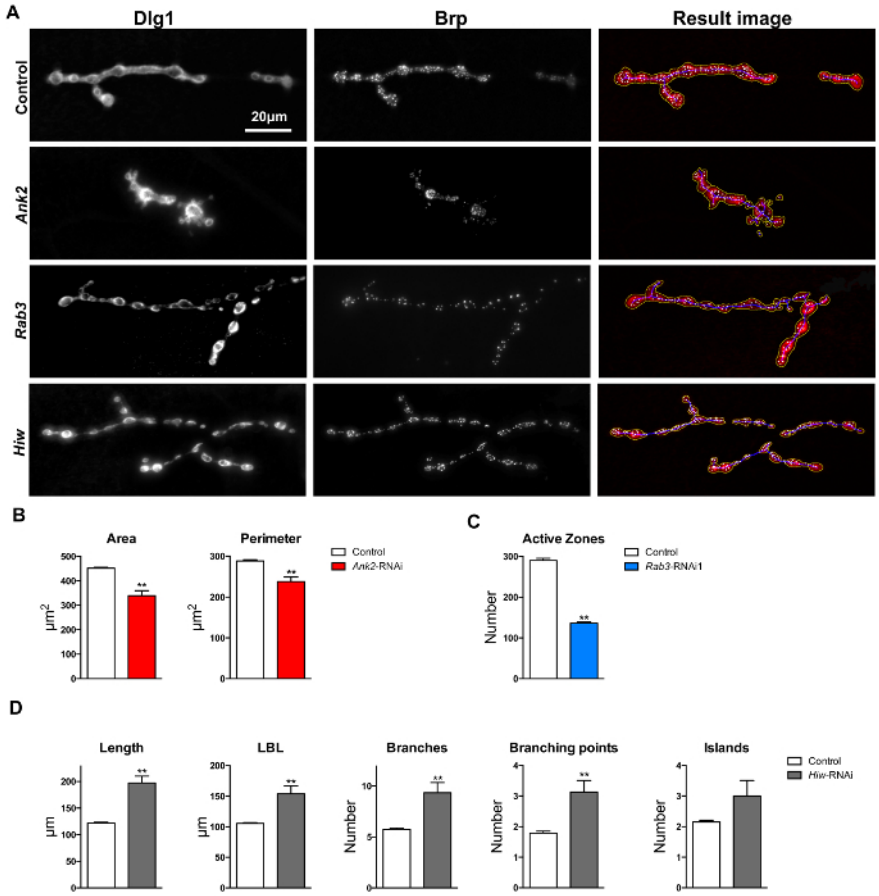


**Figure 6: Macro Assessment and Quantification of NMJs on Muscle 4.** (**A**) Result images after running "*Drosophila* NMJ Morphometrics" macro on Dlg-1 and Brp immunolabeled NMJ terminals. Parameters area, perimeter and boutons are represented by the macro-annotated yellow outline. Parameters length, longest branch length (LBL), branches, branching points, and islands are presented by the macro-annotated blue outline. Brp-immunolabeled foci (active zones) are represented by the macro as white spots in the result images. The scale bar indicates 20 µm. (**B**) *Ankyrin2* RNAi knockdown exhibit a smaller NMJ area and perimeter compared to genetic background controls. (**C**) *Rab3* knockdown resulted in NMJs with a lower number of Brp-positive active zones compared to genetic background controls. (**D**) *Highwire* knockdown resulted in longer, higher longest branch length, more branched and with more branching points per NMJ terminals compared to genetic background control NMJs. Error bars indicate SEM, ** $p < 0.01$, two tailed T-test. Please click here to view a larger version of this figure.

| Parameter | NMJ structure | Explanation |
|---|---|---|
| Area (µm2) | NMJ outline | The area of the complete labelled NMJ |
| Perimeter (µm) | NMJ outline | The perimeter belonging to the area |
| #Boutons | NMJ outline | The number of synaptic boutons ('pearls on a string') of the NMJ |
| Length (µm) | Skeleton | The total length of the complete NMJ terminal |
| Longest branch length (µm) | Skeleton | The sum of the length of the longest continuous path connecting any two endpoints of the NMJ |
| #Branches | Skeleton | The total number of branches |
| #Branching points | Skeleton | The number of branching points (several branches can derive from one branching point) |
| #Islands | Skeleton | The number of non-connected Dlg1-positive synaptic compartments (or any other staining) |
| #Active zones | Brp-positive spots | The number of active zones, based on Brp staining |

**Table 1: NMJ Parameters Measured by "*Drosophila* NMJ Morphometrics".** The NMJ parameters measured by the "*Drosophila* NMJ Morphometrics" macro will appear as a list in the obtained text file, following the order described in this table. This table is reprinted from Nijhof *et al.*[17]

| Parameter | NMJ structure | Explanation |
|---|---|---|
| Boutons | NMJ outline | The number of synaptic boutons ('pearls on a string') of the NMJ |
| Bouton area | NMJ outline | The total area of all boutons |
| Length (µm) | Skeleton | The total length of the complete NMJ terminal |
| Longest branch length (µm) | Skeleton | The sum of the length of the longest continuous path connecting any two end points of the NMJ |
| #Branches | Skeleton | The total number of branches |
| #Branching points | Skeleton | The number of branching points (several branches can derive from one branching point) |
| #Islands | Skeleton | The number of non-connected Dlg1-positive synaptic compartments (or any other staining) |
| #Active zones | Brp-positive spots | The number of active zones, based on Brp staining |

**Table 2: NMJ Parameters Measured by "*Drosophila* NMJ Bouton Morphometrics".** The NMJ parameters measured by the "*Drosophila*_Bouton_NMJ_Morphometrics" macro will appear as a list in the obtained text file, following the order described in this table. This table is reprinted from Nijhof *et al.*[17]

| Segmentation | Observed errors | Example | Required adjustments | |
|---|---|---|---|---|
| NMJ Area and perimeter (Represented by yellow outline in result image) | Parts of the synaptic terminal are either not included in the yellow outline or parts of the background are included in the synaptic terminal outlined in yellow. | **Figure 5A-B** | Adjust 'Rolling Ball Radius' value. See section 6.1. | Adjust 'NMJ outline threshold'. See section 6.2. |
| NMJ length related parameters (Represented by blue skeleton line in the results image) | Blue skeleton line either extends beyond or is not present along the entire synaptic terminal. | **Figure 5C-D** | Adjust 'Rolling Ball Radius' value. See section 6.1. | Adjust 'NMJ outline threshold'. See section 6.2. |
| Brp-positive puncta (Represented by dots in results image) | Too many active zones are detected. | **Figure 5E-E'** | Decrease the 'Find maxima noise tolerance' value. See section 6.5. | |
| Brp-positive puncta (Represented by dots in results image) | Active zones are missed by the analysis. | **Figure 5G-G'** | Increase the 'Find maxima noise tolerance' value. See section 6.5. | Decrease 'Brp-puncta lower threshold'. See section 6.6. |
| Brp-positive puncta (Represented by dots in results image) | Active zone artifacts are detected outside of the synaptic terminal. | **Figure 5F** | Adjust 'Active Zone threshold' section 6.2. | Increase 'Brp-puncta lower threshold'. See section 6.6. |
| Small particles | Particles such a crystals or dust that are part of the background appear to be included in the segmentation. | **Figure 5J** | Select the box 'Remove small particles'. See section 6.3. | Determine small particles maximum size. See section 6.3. |
| Bouton segmentation | Incorrect bouton segmentation (Only applicable to Drosophila NMJ Bouton Morphometrics; do not use Drosophila NMJ Morphometrics for bouton segmentation). | **Figure 5H-I** | Adjust 'NMJ outline threshold'. See section 6.1. | Determine 'minimum bouton size'. See section 6.4. |

**Table 3: Troubleshooting Guide for the Different Kinds of Errors in Image Segmentation that can be Produced by the Macros.** This table describes different kinds of image segmentation errors produced by the macros. These can easily be detected in the results images. Examples of each error type are shown in **Figure 4**. In the "adjustments section" of the table, the settings that need to be adjusted are highlighted, and the user is referred to the critical sub-step of section 6, which describe how to adjust these settings.

## Discussion

"*Drosophila* NMJ Morphometrics" and "*Drosophila* NMJ bouton Morphometrics" are powerful tools for researchers interested in evaluating synapse morphology. Manual assessment of NMJ parameters is laborious; it is estimated that the macros would save an experienced researcher up to 15 min/NMJ spent on manual image segmentation. With one to two dozens of synapses evaluated per condition or genotype, this quickly sums up to considerable amounts of saved time, even in small scale studies. When performing large screens, the gain of using high throughput analysis, compared to manual assessment and quantification, can be immense. In addition to increased throughput, the macros readily provide objective analysis; they exclude personal biases that otherwise require blinded experiments as well as interpersonal differences that occur when multiple researchers are involved in the analysis. Finally, the macros provide a sensitive and accurate analysis of NMJ features, allowing the identification of synaptic regulators that cause rather subtle than dramatic NMJ defects and have so far remained unappreciated by the researcher's eye. Detailed information about validation procedures and the algorithms utilized in the macros are found in the publication Nijhof *et al.*[17].

The functionality of the macros has been validated to appropriately measure morphological features of *Drosophila melanogaster* NMJs at muscle 4. Subsequently, it was demonstrated that the macros were also suitable to analyze synapses at other muscles in this organism. It is likely that the macros can also be used to measure morphological parameters of NMJ with similar structure in other species, including other *Drosophila* species and further insects. Even NMJs very distant in evolution, *e.g.,* NMJs of mice, show a quite similar structural conformation[29]. The macros have not been tested on NMJ preparations from other species but potential users are encouraged to test the macros for such purposes.

It is very important that the user explores the different auto-thresholds and algorithms to define/choose the most suitable macro settings for the images. With these settings, an accuracy of approximately 95% is achieved when macro assessment was compared to manual evaluation. Adjusting the macro settings to properly segment 100% of the images can be a very laborious or even impossible procedure. Therefore, exclusion of images not properly segmented is recommended if their numbers are below 5%. Evidently, if the quality of the images is low, the macros will generate higher ratios of unsatisfactory image segmentations. Low quality images will similarly influence manual evaluation and can therefore not be linked to the performance of the macros. Nonetheless the macros are rather robust as they were designed for images generated on a high content microscope (an automated fluorescence microscope that allows imaging of large numbers of samples)[17].

A critical point is that the user visually inspects all result images generated by the macros. This will allow to detect and exclude pictures with unsatisfying segmentation. In section 6 of this protocol, the user is guided how to adjust the settings for correct image segmentation when running the sub-macro "Analyze". To quickly familiarize with the requirements of the macros and how to adjust the macro settings a folder called "Examples_adjusting macro settings" is included in the macro repository https://doi.org/10.6084/m9.figshare.2077399.v1. Thirteen subfolders, each with examples images obtained at different microscope platforms (high content/confocal/fluorescence microscopes) and different immunostainings, are provided. A PDF entitled “Examples guide” is included in the same folder where the settings required for each example are provided, along with a text document providing the expected results and results images.

The macros were designed to process images saved as .tiff separated files, nonetheless some users might have saved their images in a different format. The following website https://doi.org/10.6084/m9.figshare.2077399.v1[21] contains a folder named "*Drosophila* NMJ" where three example files (Example 1 - 3) and the document "Examples Guide" with detailed instructions how to import images into the macro if not stored as .tiff separated files can also be found in the same folder.

Together, "*Drosophila* NMJ Morphometrics" and "*Drosophila* NMJ bouton Morphometrics" macros quantify ten different NMJ features: NMJ area, NMJ perimeter, number of boutons, NMJ bouton area, NMJ length, NMJ longest branch length, number of islands, number of branches, number of branching points and number of active zones. This provides a great advantage over so far available tools that can assess only one or a few synaptic features[30,31]. Multiparametric quantitative analysis bears great potential for new discoveries, *e.g.,* to identify novel regulators that control one up to numerous aspects of synapse biology. It also provides the required resolution to determine genes that coregulate exactly the same or overlapping NMJ features and thus are likely to operate in common molecular pathways. Finally, it opens the possibility to investigate how different synaptic parameters correlate with one another in undisturbed conditions[17] and which genes ensure such coordinated morphometric correlations.

Taken together, this protocol illustrates how to use the two macros "*Drosophila* NMJ Morphometrics" and "*Drosophila* NMJ Bouton Morphometrics", which perform objective and sensitive quantification of ten morphological NMJ features in a high-throughput manner.

## Disclosures

The authors have no conflicts of interest to disclose.

## Acknowledgements

We acknowledge the Vienna *Drosophila* Resource Center and Bloomington Drosophila stock center (NIH P40OD018537)for providing *Drosophila* strains. We thank Jack Fransen from the Microscopical Imaging Centre for expert support in imaging. This study was supported by VIDI and TOP grants (917-96-346, 912-12-109) from the Netherlands Organization for Scientific Research (NWO), by two DCN/Radboud University Medical Center PhD fellowships, by the German Mental Retardation Network funded by the NGFN+ program of the German Federal Ministry of Education and Research (BMBF) and by the European Union's FP7 large scale integrated network Gencodys (HEALTH-241995) to AS. The funders had no role in study design, data collection and analysis, decision to publish, or preparation of the manuscript.

## References


1. Lin, Y. C., & Koleske, A. J. Mechanisms of synapse and dendrite maintenance and their disruption in psychiatric and neurodegenerative disorders. *Annu Rev Neurosci.* **33**, 349-378 (2010).
2. van Bokhoven, H. Genetic and epigenetic networks in intellectual disabilities. *Annu Rev Genet.* **45**, 81-104 (2011).
3. Penzes, P., Buonanno, A., Passafaro, M., Sala, C., & Sweet, R. A. Developmental vulnerability of synapses and circuits associated with neuropsychiatric disorders. *J Neurochem.* **126**, 165-182 (2013).
4. Mainen, Z. F., & Sejnowski, T. J. Influence of dendritic structure on firing pattern in model neocortical neurons. *Nature.* **382**, 363-366 (1996).
5. Yuste, R., Majewska, A., & Holthoff, K. From form to function: calcium compartmentalization in dendritic spines. *Nat Neurosci.* **3**, 653-659 (2000).
6. Vetter, P., Roth, A., & Hausser, M. Propagation of action potentials in dendrites depends on dendritic morphology. *J Neurophysiol.* **85**, 926-937 (2001).
7. Bosch, M., & Hayashi, Y. Structural plasticity of dendritic spines. *Curr Opin Neurobiol.* **22**, 383-388 (2012).
8. Mehnert, K. I., & Cantera, R. Circadian rhythms in the morphology of neurons in Drosophila. *Cell Tissue Res.* **344**, 381-389 (2011).
9. Sigrist, S. J., Reiff, D. F., Thiel, P. R., Steinert, J. R., & Schuster, C. M. Experience-dependent strengthening of Drosophila neuromuscular junctions. *J Neurosci.* **23**, 6546-6556 (2003).
10. Ruiz-Canada, C., & Budnik, V. Introduction on the use of the Drosophila embryonic/larval neuromuscular junction as a model system to study synapse development and function, and a brief summary of pathfinding and target recognition. *Int Rev Neurobiol.* **75**, 1-31 (2006).
11. Menon, K. P., Carrillo, R. A., & Zinn, K. Development and plasticity of the Drosophila larval neuromuscular junction. *Wiley Interdiscip Rev Dev Biol.* **2**, 647-670 (2013).
12. Kraut, R., Menon, K., & Zinn, K. A gain-of-function screen for genes controlling motor axon guidance and synaptogenesis in Drosophila. *Curr Biol.* **11**, 417-430 (2001).
13. Parnas, D., Haghighi, A. P., Fetter, R. D., Kim, S. W., & Goodman, C. S. Regulation of postsynaptic structure and protein localization by the Rho-type guanine nucleotide exchange factor dPix. *Neuron.* **32**, 415-424 (2001).
14. Eaton, B. A., Fetter, R. D., & Davis, G. W. Dynactin is necessary for synapse stabilization. *Neuron.* **34**, 729-741 (2002).
15. Laviolette, M. J., Nunes, P., Peyre, J. B., Aigaki, T., & Stewart, B. A. A genetic screen for suppressors of Drosophila NSF2 neuromuscular junction overgrowth. *Genetics.* **170**, 779-792 (2005).
16. Collins, C. A., Wairkar, Y. P., Johnson, S. L., & DiAntonio, A. Highwire restrains synaptic growth by attenuating a MAP kinase signal. *Neuron.* **51**, 57-69 (2006).
17. Nijhof, B. *et al.* A New Fiji-Based Algorithm That Systematically Quantifies Nine Synaptic Parameters Provides Insights into Drosophila NMJ Morphometry. *PLoS Comput Biol.* **12**, e1004823 (2016).
18. Schindelin, J. *et al.* Fiji: an open-source platform for biological-image analysis. *Nat Methods.* **9**, 676-682 (2012).
19. Brent, J. R., Werner, K. M., & McCabe, B. D. Drosophila larval NMJ dissection. *J Vis Exp.* (2009).
20. Dubos, A. *et al.* Conditional depletion of intellectual disability and Parkinsonism candidate gene ATP6AP2 in fly and mouse induces cognitive impairment and neurodegeneration. *Hum Mol Genet.* **24**, 6736-6755 (2015).
21. Nijhof, B. *et al. Drosophila NMJ Morphometrics.* figshare. < https://doi.org/10.6084/m9.figshare.2077399.v1> (2017).
22. Ferreira, T., & Rasband, W. *ImageJ User Guide IJ 1.46.* <http://rsbweb.nih.gov/ij/docs/guide/146-29.html> (2014).
23. Ferreira, T., & Rasband, W. *ImageJ User Guide IJ 1.46.* <http://fiji.sc/Auto_Threshold> (2014).
24. Pielage, J. *et al.* A presynaptic giant ankyrin stabilizes the NMJ through regulation of presynaptic microtubules and transsynaptic cell adhesion. *Neuron.* **58**, 195-209 (2008).
25. Koch, I. *et al.* Drosophila ankyrin 2 is required for synaptic stability. *Neuron.* **58**, 210-222 (2008).
26. Iqbal, Z. *et al.* Homozygous and heterozygous disruptions of ANK3: at the crossroads of neurodevelopmental and psychiatric disorders. *Hum Mol Genet.* **22**, 1960-1970 (2013).
27. Prokop, A. Organization of the efferent system and structure of neuromuscular junctions in Drosophila. *Int Rev Neurobiol.* **75**, 71-90 (2006).
28. Wan, H. I. *et al.* Highwire regulates synaptic growth in Drosophila. *Neuron.* **26**, 313-329 (2000).
29. Shi, L., Fu, A. K., & Ip, N. Y. Molecular mechanisms underlying maturation and maintenance of the vertebrate neuromuscular junction. *Trends Neurosci.* **35**, 441-453 (2012).
30. Sutcliffe, B., Forero, M. G., Zhu, B., Robinson, I. M., & Hidalgo, A. Neuron-type specific functions of DNT1, DNT2 and Spz at the Drosophila neuromuscular junction. *PLoS One.* **8**, e75902 (2013).
31. Carpenter, A. E. *et al.* CellProfiler: image analysis software for identifying and quantifying cell phenotypes. *Genome Biol.* **7**, R100 (2006).